A NUMERICAL ANALYSIS OF FLOW AND DISPERSION AROUND A CUBE

Thomas J Scanlon
Department of Mechanical Engineering
University of Strathclyde
Glasgow G1 1XJ
Scotland

ABSTRACT

This work describes the computational fluid dynamic (CFD) simulation of flow and pollutant dispersion around a cube. The work attempts to model the characteristics of an atmospheric boundary layer type flow over a building which has a pollutant source at its roof centre. For the flow field, two different numerical schemes for the discretisation of convection have been employed namely the second order accurate QUICK scheme and the first order HYBRID-UPWIND scheme. The results for the velocity field appear to be inconclusive with reference to the merits of each of the schemes employed. Different regions of the flow appear to profit from the application of each scheme and, although the general flow field is reasonably well predicted, it is suggested that the inadequacies of the turbulence model employed may outweigh any benefits to be gained from the implementation of a higher order convection scheme. For the pollutant dispersion, variations in the turbulent Schmidt number in accordance with previously published work appear to improve the prediction of pollutant concentrations.

INTRODUCTION

The analysis of flow and dispersion of a pollutant source around a building in an atmospheric boundary layer is important from a scientific and environmental viewpoint. Various authors have conducted both physical and/or numerical studies of such flows (Robins and Castro-I (1977), Robins and Castro-II (1977), Dawson, Stock and Lamb (1991), Murakami and Mochida (1988) and Paterson and Apelt (1990)). The most notable experimental study has been that of Robins and Castro-I and II (1977) in which the authors have simulated an atmospheric boundary layer flow over a model building within a wind-tunnel. From this and other works it is noted that flows within the vicinity of large buildings are extremely complicated in nature, containing strong pressure gradients, acute streamline curvature, separation, reattachment, high turbulence intensities and recirculation zones. Such flows thus represent a significant challenge to any numerical model. The experiments of Robins and Castro-II (1977) also considered the release of a neutrally buoyant pollutant from the centre of the roof of the model cube and pressure coefficients, velocities, turbulence parameters and species concentrations were obtained. This work has provided the basis for much numerical comparison work over the last 10 or so years.

Computational work in this field has concentrated principally on the prediction of the flow field around three dimensional blockages within an atmospheric boundary layer (Richards (1989), Murakami and Mochida (1988), Paterson and Apelt (1989)). In these works the authors have computed the flow and turbulence fields around the blockage for an angle of attack of 0^o to the upwind face of the building and pollutant dispersion has not been considered. Common conclusions within these papers are that the flow field can be reasonably well predicted although the inadequacies of the isotropic two-equation k-ε turbulence model means that turbulence fields are limited accuracy. Murakami *et al* (1992) sought to overcome such inadequacies by employing other turbulence models ASM, LES with some success although other problems were encountered such as over estimation of the dissipation rate of turbulence kinetic energy in the recirculation zone in the wake of the body.

Only a limited amount of numerical work involving pollutant dispersion appears to have been carried out, Dawson, Stock and Lamb (1991), Zhang *et al* (1992) and Dargent (1996). In these works the flow field around the blockage has been sufficiently estimated that the transport characteristics (convection, diffusion) for the scalar pollutant could be derived from it. Such transport characteristics would be appropriate for passive scalar transport, however, all of the above authors have investigated changes in the turbulent Schmidt number for the transported pollutant in accordance with physical observations in an atmospheric boundary layer. This has resulted in Schmidt numbers altered from the conventional value of σ = 1.0 for all coordinate directions to typical values of σ_y=0.55, σ_x=0.77 and σ_z=0.77. Such variations were observed to improve pollutant diffusion transport.

In considering flow around a bluff body such as a cube it is important to accurately capture the shear layers as they separate from the upstream edges of the body and form a horseshoe type vortex in the downstream wake. The possibility exists of excess smearing of the shear layer profile with the use of the first-order accurate UPWIND (Patankar,1980) scheme for the discretisation of convective transport at cell Peclet numbers greater the 2. Such smearing exists due to the increase in the magnitude of multidimensional false diffusion errors as a consequence of the implementation of the UPWIND scheme. De Vahl Davis and Mallinson (1972) have provided an estimate of the false diffusion coefficient for two dimensional flows, this being

$$\Gamma_{false} = \frac{\rho U \Delta x \Delta y \sin 2\theta}{4\left(\Delta y \sin^3\theta + \Delta x \cos^3\theta\right)} \qquad (1)$$

The false diffusion errors manifest themselves as an artificial increase in the diffusion of the conserved species normal to the streamlines with the maximum error occurring at 45^o. Many alternative schemes have been proposed in order to reduce Γ_{false} such as the widely used QUICK scheme of Leonard (1979) and flow-oriented type algorithms such as CUPID (Patel et al, 1985) and SUCCA (Carey et al, 1993). The QUICK scheme has been found to be non-bounding under certain circumstances while the SUCCA scheme possesses stability problems when applied to momentum transport. The CUPID scheme has been applied only to scalar convective transport.

In this paper an angle of attack of 45^o has been chosen as this represents the worst case scenario for a study of the effects of numerical diffusion and also for the fact that there appears to be no literature carried out for this case. The effects of first order upwinding are presented and discussed in relation to the analysis of three dimensional flow over a cube in an atmospheric boundary layer. Two convection algorithms are implemented - HYBRID-UPWIND (Patankar, 1980) and QUICK - for the discretisation of convective momentum transport and comparisons are made between the two schemes for prediction of the velocity and turbulence fields in the vicinity of the blockage. For the pollutant dispersion around the cube, variations in the turbulent Schmidt number in accordance with previous work have been employed in order to improve the estimates of pollutant concentration in the wake of the blockage. All numerical data is compared with the experimental wind tunnel results of Robins and Castro

NUMERICAL MODEL

Geometrical configuration

The geometrical model for the atmospheric boundary layer flow over the cube is shown in Figure 1.

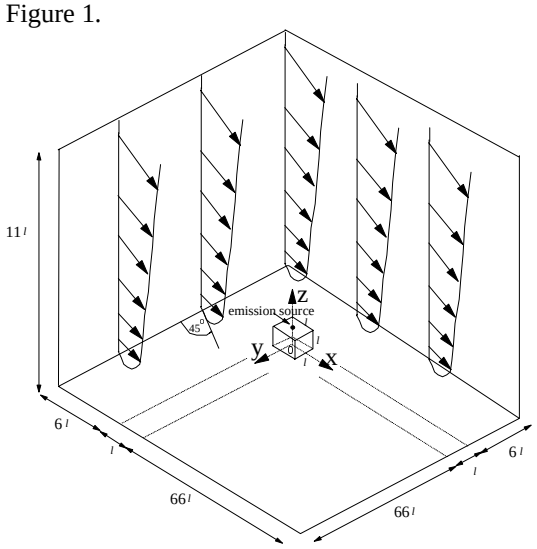

Figure 1 *Geometry of Robins and Castro used as test case.*

The geometry is identical to that examined experimentally in a wind tunnel by Robins and Castro where a cube of equivalent length, width and height l = 0.2m is placed in a simulated atmospheric boundary layer flow of height H = 2.0 m. The cube was placed on a ground plane as shown in Figure 1 and this configuration represented typical environmental conditions for a 60m high building in a 600m high boundary layer.

The computational mesh employed was a conventional non-uniform mesh for which the number of grid cells was 73X by 73Y by 33Z cells and a typical grid configuration in the region of the cube is shown in Figure 2

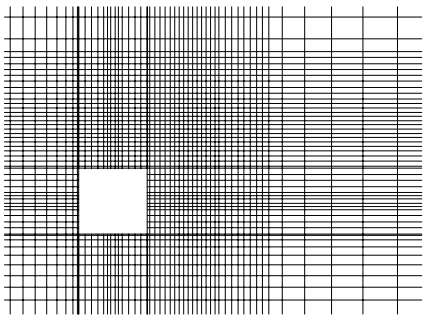

Figure 2 *Computational mesh in region of cube.*

Governing equations

The fluid flow was modelled by partial differential equations describing the conservation of mass, momentum and species concentration in three rectangular Cartesian coordinate directions for steady, incompressible flow which, after Reynolds averaging become:

Conservation of mass

$$\frac{\partial U_i}{\partial x_i} = 0 \qquad (2)$$

Conservation of momentum

$$\frac{\partial U_i U_j}{\partial x_j} = -\frac{\partial}{\partial x_i}\left(\frac{P}{\rho} + \frac{2}{3}k\right) + \frac{\partial}{\partial x_j}\left\{\nu_t\left(\frac{\partial U_i}{\partial x_j} + \frac{\partial U_j}{\partial x_i}\right)\right\} \qquad (3)$$

Conservation of scalar species

$$\frac{\partial C U_i}{\partial x_j} = \frac{\partial}{\partial x_j}\left\{\frac{\nu_t}{\sigma_{c,j}}\frac{\partial C}{\partial x_j}\right\} \qquad (4)$$

Transport equation for k

$$\frac{\partial k U_i}{\partial x_j} = \frac{\partial}{\partial x_j}\left\{\frac{\nu_t}{\sigma_1}\frac{\partial k}{\partial x_j}\right\} + \nu_t S - \varepsilon \qquad (5)$$

Transport equation for ε

$$\frac{\partial \varepsilon U_i}{\partial x_j} = \frac{\partial}{\partial x_j}\left\{\frac{\nu_t}{\sigma_2}\frac{\partial \varepsilon}{\partial x_j}\right\} + C_1\frac{\varepsilon}{k}\nu_t S - C_2\frac{\varepsilon^2}{k} \qquad (6)$$

where

$$\nu_t = C_\mu \frac{k^2}{\varepsilon}$$

$$S = \left(\frac{\partial U_i}{\partial x_j} + \frac{\partial U_j}{\partial x_i}\right)\frac{\partial U_i}{\partial x_j}\ ,\ \sigma_1 = 1.0\ ,\ \sigma_2 = 1.3$$

$$C_\mu = 0.09\ ,\ C_1 = 1.44$$

$$C_2 = 1.92\ ,\ \sigma_{c,j} = 1.0$$

It should be noted that $\sigma_{c,j}$ is the direction-dependent turbulent Schmidt number for the species equation which may be varied according to pollutant dispersion observations within the atmospheric boundary layer.

Solution algorithm

The CFD code used was the commercially available finite volume based package PHOENICS. For the discretisation of convective transport the HYBRID-UPWIND scheme is the default scheme within the PHOENICS code and the QUICK scheme was also used as an alternative. For the pressure-velocity coupling the code employs a global solver based on the SIMPLE (Patankar, 1980) algorithm.

Boundary conditions

All boundary conditions were implemented by the inclusion of additional source and/or sink terms in the finite volume equations for the computational cells at the domain boundaries. At the upwind free boundary an inlet velocity profile for the atmospheric boundary layer was applied. This profile was based on a curve fitted through the experimental data of Robins and Castro as shown below in Figure 3. The numerical curve possessed the following form:

$$\frac{z}{l} = 0.0362e^{5.95\frac{U}{U_{ref}}} \qquad (7)$$

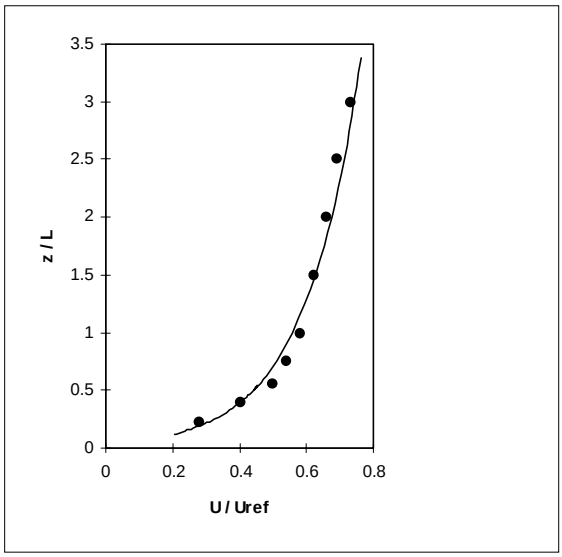

Figure 3 *Inlet atmospheric boundary layer profile (____ : numerical profile, ● exp: Robins and Castro (1977))*

Inlet values of the turbulence parameters k and ε were also prescribed pertaining to the experimental results of Robins and Castro.

At the downwind and upper free boundaries a constant pressure boundary condition was applied. For the cube surfaces the standard form of the log-law wall function was applied while at ground level a roughness height $z_0 = 0.0022l$ was introduced such that at ground level:

$$U = \frac{u_*}{\kappa} ln \frac{z}{z_o} \qquad (8)$$

For the turbulence quantities k and ε the following relationships were applied at solid regions

$$k = \frac{u_*^2}{\sqrt{C_\mu}}, \quad \varepsilon = \frac{u_*^3}{\kappa z} \qquad (9)$$

Convergence criteria

The solution was declared converged when the sum of the mass, momentum and species residues were less than a residual factor of 0.01 times the incoming mass flow. It was found that the total solution time was of the order of 12 hours using a Pentium 133 computer.

ANALYSIS

The velocity field

In the first instance we will consider the general allure of the flow field around the bluff body. Figure 4 shows a plan view of the flow field close to the ground level and we may observe the twin symmetrical vortices that form part of complex three-dimensional bubble in the immediate wake of the cube.

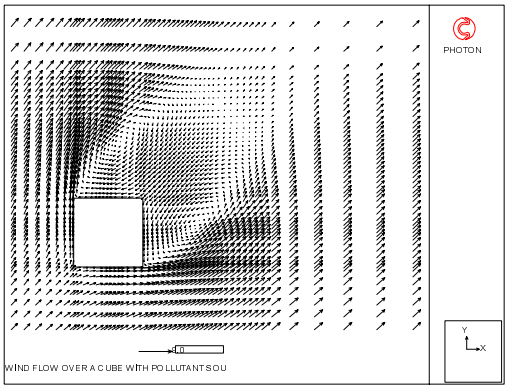

Figure 4 *Plan view of velocity vectors around cube showing twin symmetrical vortices in wake.*

Taking a horizontal slice through the mid-plane of the cube (y = 0) we observe the three dimensional nature of the wake region immediately downstream of the blockage where a large horseshoe-type vortex appears at the right-hand edge of the cube.

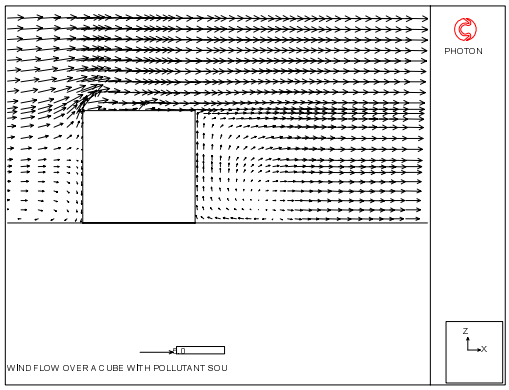

Figure 5 *Elevation of velocity vectors around cube showing the three-dimensional nature of the flow.*

The following Figures 6 to 10 show the velocity profiles at various regions within the flow and we may make a comparison between the velocities predicted using the different numerical convection schemes HYBRID-UPWIND and QUICK and the experimental results of Robins and Castro.

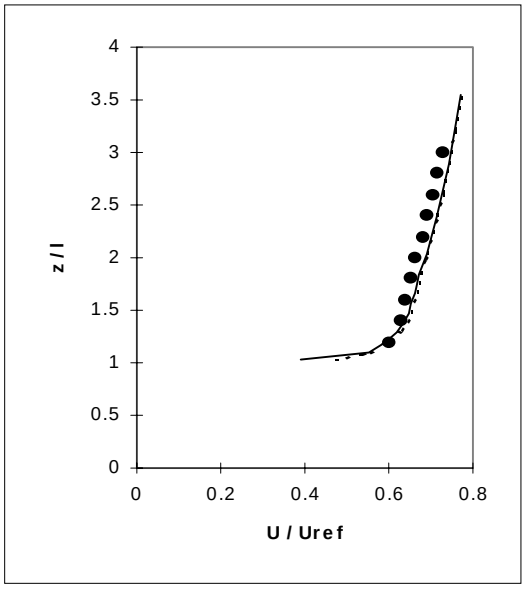

Figure 6 *Velocity profile in cross-diagonal downwind direction at x/l = 0 (____ : numerical profile UPWIND, ----- numerical profile QUICK, ● exp: Robins and Castro (1977))*

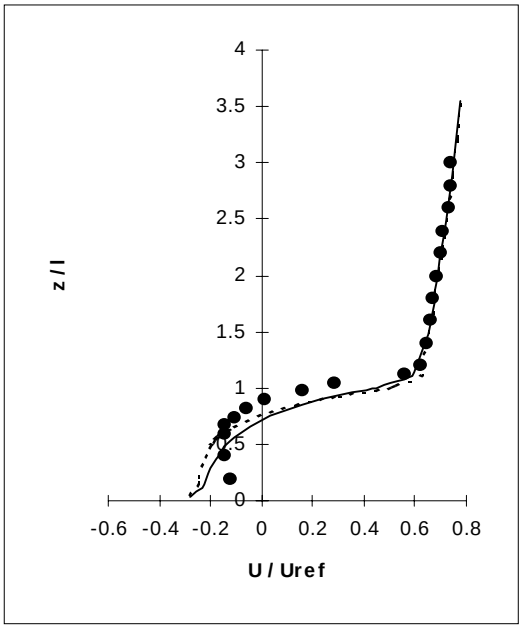

Figure 7 *Velocity profile in cross-diagonal downwind direction at x/l = 1 (____ : numerical profile UPWIND, ----- numerical profile QUICK, ● exp: Robins and Castro (1977))*

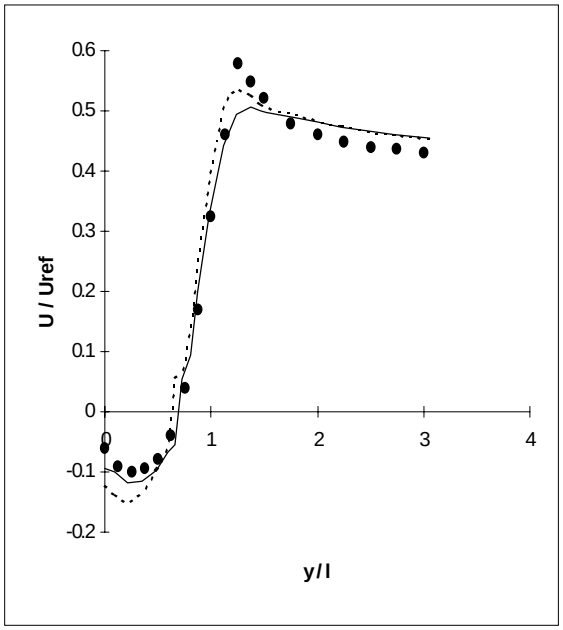

Figure 9 *Velocity profile in spanwise direction at mid-height of cube and x/l = 0.75 (____ : numerical profile UPWIND, ----- numerical profile QUICK, ● exp: Robins and Castro (1977))*

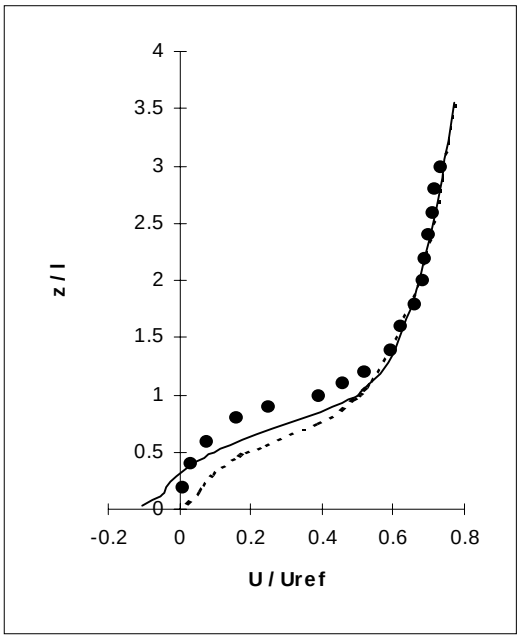

Figure 8 *Velocity profile in cross-diagonal downwind direction at x/l = 2 (____ : numerical profile UPWIND, ----- numerical profile QUICK, ● exp: Robins and Castro (1977))*

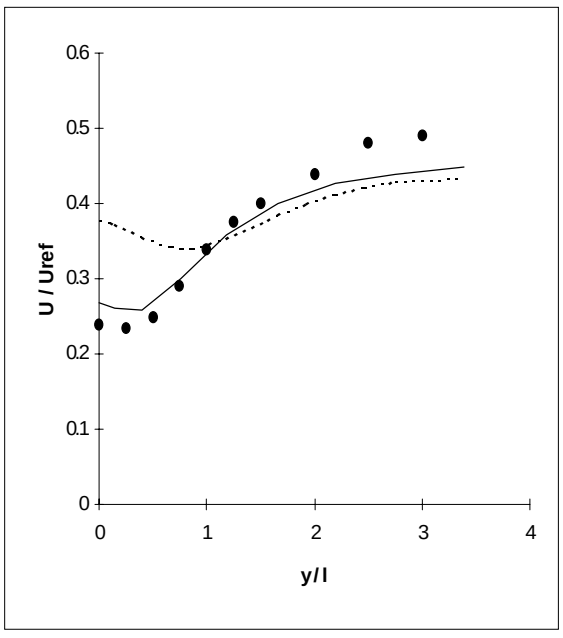

Figure 10 *Velocity profile in spanwise direction at mid-height of cube and x/l = 3.0 (____ : numerical profile UPWIND, ----- numerical profile QUICK, ● exp: Robins and Castro (1977))*

As can be observed in Figures 6 to 10 the general flow characteristics appear to have been captured by the numerical model. For the velocity profile at the cube centre shown in Figure 6 there is only a marginal difference in the results for UPWIND and QUICK. Very little numerical diffusion exists at this location as there is negligible spanwise shear in this region. However, in the downstream wake, larger velocity gradients appear and the differences between the solutions using UPWIND and QUICK become rather more apparent.

In Figure 7 the velocity profile relating to the computational cells immediately downstream of the cube corner appears to have been more accurately captured using QUICK. However, both schemes show an overestimation of the negative recirculation velocities towards ground level.

In Figure 8 for the velocity profile at the diagonal distance $x/l = 2.0$ it is now the UPWIND prediction that appears to more accurately capture the flow characteristics, although the UPWIND prediction does promote a slight overprediction of negative recirculating velocities. Both UPWIND and QUICK perform well in the upper reaches of the wake ($x/l > 1$) although this might be anticipated as velocity gradients and hence mean shear levels will be low at this region.

For the spanwise velocity profiles of Figures 9 and 10 the UPWIND scheme appears to out-perform its QUICK counterpart. The general observation being that the QUICK solution tends to overestimate the velocity profiles, perhaps as a consequence of its non-bounding characteristics, while the UPWIND solution, being numerically dissipative, underestimates the velocity field.

It is important to point out, however, that the diffusion characteristics of the flow equations strongly depend on the turbulence model applied. In this instance, the two-equation k-ε model has been employed. This model relies on the assumption that the flow is highly turbulent and that normal stress isotropy exists in the flow. However, both in the atmospheric boundary layer upstream of the cube and in the recirculating wake downstream the flow is by no means isotropic (Paterson and Apelt (1989), Robins and Castro (1977)) thus such a model cannot predict the directional dependency of the turbulent stresses. This implies that errors will exist in the calculation of the turbulent diffusivities and a more accurate model accounting for local anisotropic turbulence such as a Reynolds Stress Model or an isotropic model accounting for streamline curvature may ameliorate the predictions. Questions remain also over the appropriateness of wall-functions at the solid boundary cells for the solution of momentum (Zhang *et al* (1992)).

The turbulence field

As has been highlighted by previous authors (Paterson and Apelt (1989), Dargent (1996)) the shortcomings of the k-ε turbulence model discussed in the previous section tends to under-predict the turbulence field. The inability of the model to account for local normal stress anisotropy is highlighted in Figures 11 to 13 which show the numerical and experimental values of the Reynolds stress component $\overline{u'u'}$ plotted in the form of a turbulent intensity. In order to avoid the possibility of predicting negative turbulent viscosities, a bounded version of the QUICK scheme known as SMART (CHAM (1996)) was employed for the convective transport of the turbulence quantities k and ε:

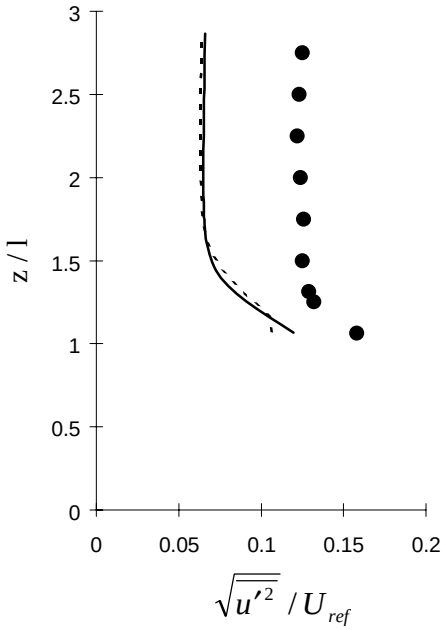

Figure 11 *Vertical profile of turbulence intensity at x/l = 0 (____ : numerical profile UPWIND, ----- numerical profile SMART, ● exp: Robins and Castro (1977))*

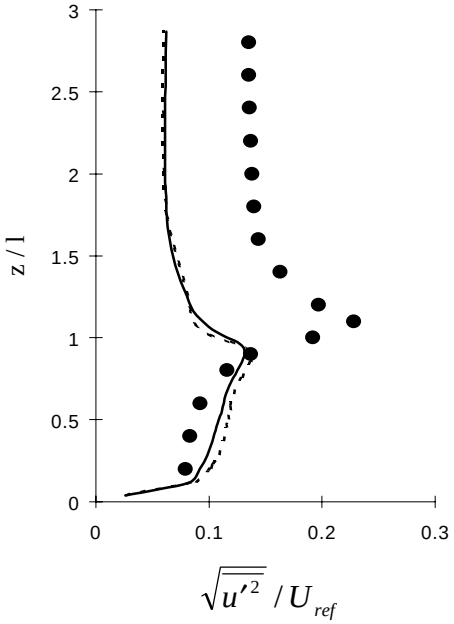

Figure 12 *Vertical profile of turbulence intensity at x/l = 1 (____ : numerical profile UPWIND, ----- numerical profile SMART, ● exp: Robins and Castro (1977))*

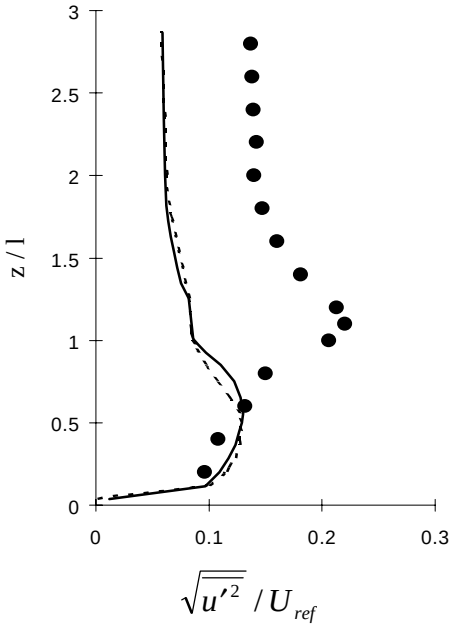

Figure 13 *Vertical profile of turbulence intensity at x/l = 2 (____ : numerical profile UPWIND, ----- numerical profile SMART, ● exp: Robins and Castro (1977))*

Figures 11, 12 and 13 highlight the fact that there appears to be little difference in the use of UPWIND or SMART for the convective transport of the turbulence quantities. This can be put down to the possible reason that the transport equations for the turbulence parameters tend to be dominated by source terms (production, dissipation) and thus the influence of altering the convection algorithm appears to be minimal.

The concentration field

In the simulation of the release of a non-reacting, neutrally buoyant pollutant at the centre of the roof of the cube we will consider the following two cases:

1) CASE A - the standard solution for the transport of scalar species with a turbulent Schmidt number $\sigma_{c,j}$ equal to 1.

2) CASE B - modification of $\sigma_{c,j}$ following the authors Dawson *et al* (1991) and Zhang *et al* (1992) who selected a modified Schmidt number equal to 0.77. After comparison with the experimental results of Robins and Castro (1977) Zhang *et al* observed also that the transversal (spanwise) diffusivity was approximately 1.4 times greater than the vertical diffusivity.

The modifications for CASE B are carried out within the transport equation for the concentration in the following manner, we may write the directional diffusion terms as:

$$D_{c,y} = \frac{\partial}{\partial y}\left(\frac{\nu_t}{\sigma_{c,y}}\frac{\partial C}{\partial y}\right) \text{with } \sigma_{c,y}= 0.77/1.4 = 0.55$$

$$D_{c,x} = \frac{\partial}{\partial x}\left(\frac{\nu_t}{\sigma_{c,x}}\frac{\partial C}{\partial x}\right) \text{with } \sigma_{c,x} = 0.77$$

$$D_{c,z} = \frac{\partial}{\partial z}\left(\frac{\nu_t}{\sigma_{c,z}}\frac{\partial C}{\partial z}\right) \text{with } \sigma_{c,z} = 0.77$$

Figures 14 to 18 show the pollutant concentration levels at various locations within the flow field:

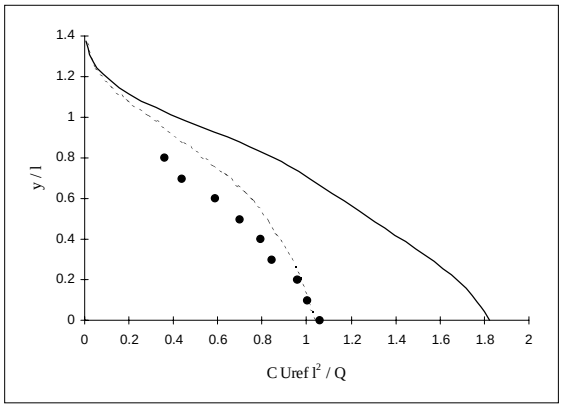

Figure 14 *Spanwise concentration profile at x/l = 0.75 and z/l = 0.45 (____ : numerical profile CASE A, ----- numerical profile CASE B, ● exp: Robins and Castro (1977))*

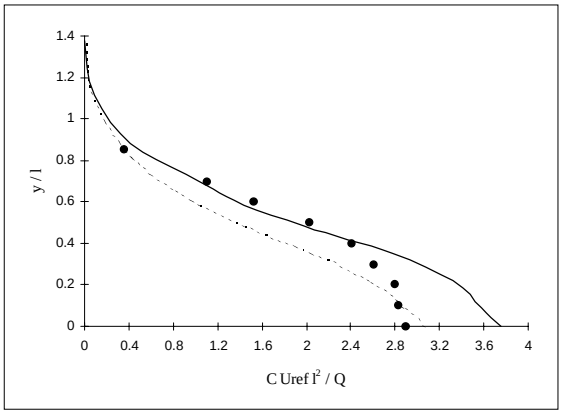

Figure 15 *Spanwise concentration profile at x/l = 0.75 and z/l = 0.85 (____ : numerical profile CASE A, ----- numerical profile CASE B, ● exp: Robins and Castro (1977))*

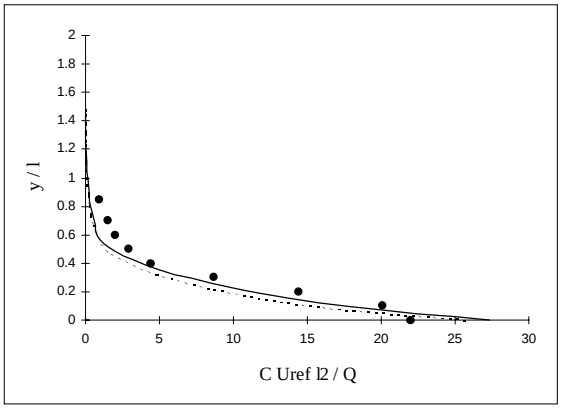

Figure 16 *Spanwise concentration profile at x/l = 0.75 and z/l = 1.05 (____ : numerical profile CASE A, ----- numerical profile CASE B, ● exp: Robins and Castro (1977))*

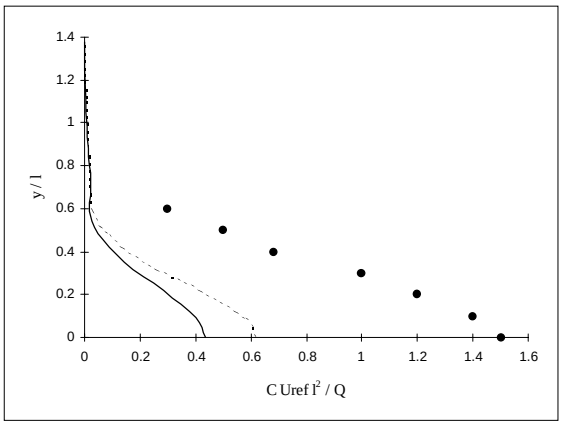

Figure 17 *Spanwise concentration profile at x/l = 0.75 and z/l = 1.25 (____ : numerical profile CASE A, ----- numerical profile CASE B, ● exp: Robins and Castro (1977))*

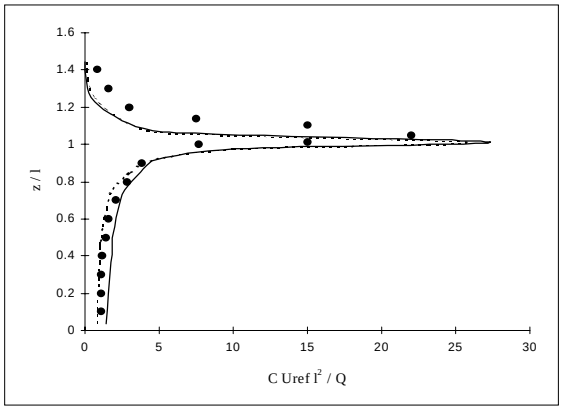

Figure 18 *Vertical concentration profile at x/l = 0.75(____ : numerical profile CASE A, ----- numerical profile CASE B, ● exp: Robins and Castro (1977))*

The UPWIND scheme has been employed for the convective transport of the pollutant. It is evident that the variations in the turbulent Schmidt number as outlined in the previous section have improved the prediction of the concentration field around the obstacle in comparison with experimental data.

CONCLUSIONS

The numerical study of flow and dispersion of a pollutant with source in the centre of the roof of the cube has been considered. The general features of the flow field appear to have been reasonably well captured. For the velocity field the results appear to be in quite close agreement with experimental data although it is unclear as to the merits of employing a higher order convection algorithm. Both the QUICK scheme and the numerically dissipative HYBRID-UPWIND alternative have been employed with the inconclusive result that different regions of the flow appear to profit from the application of each scheme. As well as numerical dissipation within the flow, inadequacies in the isotropic *k*-ε turbulence model employed may also be responsible for inaccurate prediction of all transported variables. This inability to account for local anisotropy is also a possible reason for the fact that the turbulence intensities are strongly underpredicted. For the concentration field, variations in the turbulent Schmidt number are seen to improve the overall estimates of concentration levels in comparison with experimental data.

REFERENCES

Carey, C., Scanlon, T.J. and Fraser, S.M. 'SUCCA - An Alternative Scheme to Reduce the Effects of Multidimensional False Diffusion.' *Applied Mathematical Modelling*, 17(5), pp. 263-270, May 1993.

CHAM - Polis from PHOENICS v.2.2, 1995.

Dargent, C. ' Contribution a la modelisation de la dispersion de polluants - Etude de sillages autour d'obstacles de form parallelpipedique. Ph.D Thesis, INPToulouse, 1996.

Dawson, P., Stock, D.E. and Lamb, B. 'The numerical simulation of airflow and dispersion in three-dimensional atmospheric recirculation zones', *Journal of Applied Meteorology*, Vol. 30, pp. 1005-1024, 1991.

De Vahl Davis, G. and Mallinson, G.D. 'False Diffusion in Numerical Fluid Mechanics'. *Report 1972/FMT/1*, School of Mechanical and Industrial Engineering, University of New South Wales, 1972.

Leonard, B.P. 'A Stable and Accurate Convection Modelling Procedure Based on Quadratic Upstream Interpolation.' *Computer Methods in Applied Mechanics and Engineering*, 19, pp. 59-98, 1979.

Murakami, S. and Mochida, A. '3-D numerical simulation of airflow around a cubic model by means of the *k*-ε model', *Journal of Wind Engineering and Industrial Aerodynamics*, Vol. 31, pp. 283-303, 1988.

Murakami, S., Mochida, A., Hayashi, Y. and Sakamoto, S. 'Numerical study on velocity-pressure field and wind forces for bluff bodies by *k*-ε, ASM and LES', *Journal of Wind Engineering and Industrial Aerodynamics*, Vol. 41 & 44, pp. 2841-2852, 1992.

Patankar, S.V. *Numerical Heat Transfer and Fluid Flow*, (Hemisphere, New York), 1980.

Paterson D.A. and Apelt, C.J. 'Simulation of wind flow around three-dimensional buildings', *Building and Environment*, Vol. 24, No. 1, pp. 39-50, 1989.

Paterson D.A. and Apelt, C.J. 'Simulation of flow past a cube in a turbulent boundary layer', *Journal of Wind Engineering and Industrial Aerodynamics*, Vol. 35, pp. 149-176, 1990.

Patel, M.K., Markatos, N.C. and Cross, M. Technical Note - 'Method of Reducing False-Diffusion Errors in Convection-Diffusion Problems'. *Applied Mathematical Modelling*, 9, pp. 302-306, August 1985.

Richards, P.J. ' A comparison of computer and wind-tunnel models of turbulence around the Silsoe Structures Building', *Proceedings of the First International Symposium on Computational Wind Engineering*, 1992.

Robins, A.G. and Castro, I.P. 'A wind tunnel investigation of plume dispersion in the vicinity of a surface mounted cube - I. The flow field' *Atmospheric Environment*, Vol. 11, pp. 291-297, 1977.

Robins, A.G. and Castro, I.P. 'A wind tunnel investigation of plume dispersion in the vicinity of a surface mounted cube - II. The concentration field' *Atmospheric Environment*, Vol. 11, pp. 299-311, 1977.

Zhang, Y.Q., Arya, S.P.S., Huber, A.H. and Snyder, W.H., 'Simulating the effects of upstream turbulence on dispersion around a building', Report No. EPA/600/A-92/228, US Environmental Protection Agency, Research Triangle Park, NC, 1992.

NOMENCLATURE

C	pollutant concentration
k	turbulence kinetic energy
ε	dissipation rate of k
Γ	diffusion coefficient
θ	flow angle
l	cube height
p	static pressure
Q	injection flowrate of pollutant
u,v,w,U	velocity
u_*	shear velocity
u'	fluctuating velocity
ν	kinematic viscosity
x	distance downwind of cube
y	spanwise coordinate
z	vertical coordinate
suffix	
ref	free stream
subscripts	
t	turbulent